



HAL
open science

Structural requirements of KTS-disintegrins for inhibition of $\alpha 1\beta 1$ integrin

Meghan C Brown, Johannes A Eble, Juan J Calvete, Cezary Marcinkiewicz

► **To cite this version:**

Meghan C Brown, Johannes A Eble, Juan J Calvete, Cezary Marcinkiewicz. Structural requirements of KTS-disintegrins for inhibition of $\alpha 1\beta 1$ integrin. *Biochemical Journal*, 2008, 417 (1), pp.95-101. 10.1042/BJ20081403 . hal-00479067

HAL Id: hal-00479067

<https://hal.science/hal-00479067>

Submitted on 30 Apr 2010

HAL is a multi-disciplinary open access archive for the deposit and dissemination of scientific research documents, whether they are published or not. The documents may come from teaching and research institutions in France or abroad, or from public or private research centers.

L'archive ouverte pluridisciplinaire **HAL**, est destinée au dépôt et à la diffusion de documents scientifiques de niveau recherche, publiés ou non, émanant des établissements d'enseignement et de recherche français ou étrangers, des laboratoires publics ou privés.

Structural Requirements of KTS-Disintegrins for Inhibition of $\alpha_1\beta_1$ integrin

Meghan C. BROWN*, Johannes A. EBLE†, Juan J. CALVETE‡, and Cezary MARCINKIEWICZ*.§

* Temple University, School of Medicine, Department of Biology, Center for Neurovirology, Philadelphia, PA 19122, USA

† Center for Molecular Medicine, Dept. Vascular Matrix Biology, Frankfurt University Hospital, 60590 Frankfurt-am-Main, Germany

‡ Instituto de Biomedicina de Valencia, C.S.I.C., Valencia 46010, Spain

§ To whom correspondence should be addressed. Tel.: 215-204-9561, Fax: 215-204-0679, e-mail: cmarcink@temple.edu

Running Title: KTS-disintegrin's inhibition of $\alpha_1\beta_1$ integrin

Keywords: KTS-disintegrin, obtustatin, viperistatin, integrin $\alpha_1\beta_1$ inhibitor, recombinant disintegrin, structure-function correlation.

SYNOPSIS

Obtustatin and viperistatin represent the shortest known snake venom monomeric disintegrins. We have produced recombinant full-length wild-type and site-directed mutants of obtustatin to assess the role of the ²¹KTS²³ tripeptide and C-terminal residues for specific inhibition of the $\alpha_1\beta_1$ integrin. Threonine-22 appeared to be the most critical residue for disintegrin activity, whereas substitution of flanking lysine or serine for alanine resulted in less pronounced decreased of the disintegrin's anti- $\alpha_1\beta_1$ integrin activity. The triple mutant ²¹AAA²³ was devoid of blocking activity towards $\alpha_1\beta_1$ integrin-mediated cell adhesion. The potency of recombinant KTS-disintegrins also depended on the residue C-terminally adjacent to the active motif. Substitution of wild-type obtustatin's leucine-24 for alanine slightly decreased the inhibitory activity of the mutant, whereas arginine in this position enhanced by 6-fold the potency of the mutant over wild type obtustatin. In addition, the replacements leucine-38/valine and proline-40/glutamine may account for a further 25-fold increase in $\alpha_1\beta_1$ inhibitory potency of viperistatin over KTSR-obtustatin.

INTRODUCTION

Integrins are $\alpha\beta$ heterodimeric type-I transmembrane glycoproteins that mediate a range of regulated and dynamic interactions between cells and extracellular adhesion molecules. In humans, 18 α and 8 β integrin subunits combine in a restricted manner to form at least 24 dimers, each of which exhibits a distinct ligand-binding profile [1-3]. Integrins transduce bidirectional signals across the plasma membrane, between the extracellular matrix (ECM) outside a cell and the cytoskeleton inside the cell [4,5], and integrin-mediated cell attachment to the ECM is a basic requirement to build a multicellular organism. Among the ligands of integrins are fibronectin, vitronectin, laminin, and collagen. The collagen-binding integrins ($\alpha_1\beta_1$, $\alpha_2\beta_1$, $\alpha_{10}\beta_1$, $\alpha_{11}\beta_1$) contain an approximately 200-amino-acid-residue (I- or A-) domain inserted between the second and the third Ca^{2+} -binding motifs within the N-terminal part of the α subunit that plays a central role in ligand binding [6], and play an important role in the physiology of many organs and in innate immunity, inflammation and autoimmunity [7]. The α I-domain-containing integrins that mediate direct adhesion to collagens seem to have a relatively recent history, since they have been found only in the vertebrate clade [8]. Among them, integrin $\alpha_1\beta_1$ has been recognized as a high affinity receptor for collagen type IV, and binds also, albeit with less avidity, to other collagens such as type I, XIII and XVI [9,10]. Integrin $\alpha_1\beta_1$ is highly expressed on the microvascular endothelial cells, and blocking of its adhesive properties significantly reduces the vascularization ratio and tumor growth in the mouse [11-13], suggesting potential strategies to therapeutically target these receptors to alleviate or treat disease.

Viperidae snakes have developed in their venoms an efficient and almost complete repertoire of β_1 - and β_3 -integrin receptor antagonists [14]. Thus, with the exception of the $\alpha_2\beta_1$ integrin, which is targeted by a number of C-type lectin-like proteins [15], inhibitory motifs towards β_1 and β_3 integrins have evolved in different members of the disintegrin family [16-19]. Among them, RGD blocks integrins $\alpha_8\beta_1$, $\alpha_5\beta_1$, $\alpha_v\beta_1$, $\alpha_v\beta_3$ and $\alpha_{IIb}\beta_3$; MLD targets the $\alpha_3\beta_1$, $\alpha_4\beta_1$, $\alpha_4\beta_7$, $\alpha_7\beta_1$ and $\alpha_9\beta_1$ integrins; VGD and MGD impair the function of the $\alpha_5\beta_1$ integrin; KGD inhibits the $\alpha_{IIb}\beta_3$ integrin with a high degree of selectivity; WGD has been reported to be a potent inhibitor of the RGD-dependent integrins $\alpha_5\beta_1$, $\alpha_v\beta_3$ and $\alpha_{IIb}\beta_3$; and KTS and RTS represent selective $\alpha_1\beta_1$ inhibitors [14, 20-22].

KTS/RTS-disintegrins, 41-residue monomeric polypeptides crosslinked by 4 conserved disulfide bonds, represent the shortest snake venom disintegrins described to date [13]. Disintegrin obtustatin, isolated from the venom of *Vipera lebetina obtusa*, was the first described $\alpha_1\beta_1$ antagonist [11, 23]. It blocked the adhesion of $\alpha_1\beta_1$ -expressing K562 cells to immobilized collagens IV and I with an IC_{50} of 2 nM and 0.5 nM, respectively, but was inactive against a other integrin receptors, including the $\alpha_1\beta_1$ structurally closely-related collagen receptor $\alpha_2\beta_1$ integrin. Obtustatin (5 $\mu\text{g}/\text{disk}$) inhibited 84% of FGF2-induced angiogenesis *in vivo* in the chicken [11] and the quail [24] chorioallantoic membrane assay. Moreover, in the Lewis lung [11] and B16F10 melanoma [24] syngenic mouse models, this disintegrin reduced tumor growth by about 50% and 65%, respectively, when administered intraperitoneally every other day at a dose of 5 mg/Kg. Subsequently, the KTS-disintegrins viperistatin (from *Vipera palestinae* venom) [12] and lebestatin (from *Macrovipera lebetina transmediterranea* venom [25, 26], and the RTS-disintegrin jerdostatin (recombinantly expressed by [27] from a *Protothrops jerdonii* cDNA library) have been proven to be also very potent and highly selective inhibitor of the $\alpha_1\beta_1$ integrin. NMR studies of the solution structure [28] and internal motions [29] of obtustatin have

revealed that in contrast to all known disintegrin structures in which the RGD adhesion motif is located at the apex of an eleven residue hairpin loop, the active ²¹KTS²³ tripeptide is oriented towards a side of a nine residue integrin-binding loop. The integrin binding loop of obtustatin exhibits lateral local motions within a range of approximately 35° and with maximal displacement of about 5Å, and the integrin binding loop and the C-terminal tail of the disintegrin display concerted motions in the 100-300 picosecond timescale [29]. The shape and size of its short integrin-binding loop along with its composition, flexibility, and the distinct orientation of the KTS tripeptide may underlay the structural basis of obtustatin's unique selectivity and specificity for integrin $\alpha_1\beta_1$.

Structural diversity among the $\alpha_1\beta_1$ -specific disintegrins appears to be segregated within their C-terminal halves (see Fig.3 in [13]). Viperistatin differs from obtustatin by only three amino acids at positions 24, 38 and 40, and is about 25-fold more potent than obtustatin inhibiting the interaction of human $\alpha_1\beta_1$ integrin with collagen IV *in vitro* [12]. Here we report the production and structure/function correlations of recombinant KTS-disintegrins.

EXPERIMENTAL

Antibodies, Extracellular Matrix and Cell Adhesion Proteins

Polyclonal antiserum against the snake venom disintegrin eristostatin was developed commercially (Chemicon, Temecula, CA), and the IgG fraction was purified using protein A-based purification kit (Pierce Biotechnology, Rockford, IL). Mouse anti-human β_1 integrin subunit monoclonal antibodies B44 and Lia1/2 were purchased from Chemicon and Beckman Coulter (Fullerton, CA), respectively. Goat anti-rabbit IgG conjugated with horseradish peroxidase (HRP) and alkaline phosphatase (AP) were purchased from Cell Signaling Inc. (Beverly, MA) and Sigma Inc. (St. Louis, MO), respectively. Bovine collagens type IV and type I were purchased from Chemicon and Chrono-Log Corp. (Havertown, PA), respectively. Human plasma fibronectin was from Sigma. Human VCAM-1 Ig domain was kindly provided by Dr. P. Wainreb (Biogen Inc., Cambridge, MA).

Cell Lines

K562 and Jurkat cell lines were purchased from ATCC (Manassas, VA) and cultured in RPMI 1640 and DMEM, respectively, supplemented with 10% fetal bovine serum (Gibco, Carlsbad, CA). K562 cells lines transfected with α_1 and α_2 integrins were kindly provided by Dr. M. Hemler (Dana-Farber Cancer Institute, Boston, MA) and were cultured in RPMI 1640 containing 500 $\mu\text{g}/\text{mL}$ G418 Sulfate (Mediatech Inc, Herdon, VA).

Purification of Anti-adhesive Proteins from Snake Venoms

The following snake venom proteins were purified on a C18 column eluted with a linear acetonitrile gradient using the previously described two-step reverse phase HPLC protocol [12, 30]. Disintegrins obtustatin, VLO4 and VLO5 were purified from the venom of *Vipera lebetina obtusa* purchased from Latoxan (Valence, France). Disintegrin eristostatin was isolated from *Eristocophis macmahoni* venom (Latoxan). Disintegrin viperistatin and the C-type lectin-like protein VP12 were purified from the venom of *Vipera palestinae* kindly provided by Dr. A. Bdolah (Zoology Department of Tel-Aviv University, Israel).

Cloning and Expression of Recombinant Obtustatin and its Mutants

A synthetic gene for obtustatin was designed based on the 41 amino acid sequence of obtustatin [23] and optimal codons for *E. coli* expression, and was commercially synthesized by Genscript Corp. (Piscataway, NJ). The obtustatin gene was PCR-amplified and ligated into the pGex-4-T1 vector for expression as a thrombin-cleavable glutathione S-transferase-fusion protein using the pUC57 plasmid containing the synthetic gene as a template. Forward (5'-GTTCCGCGTGGATCC TGTACGACGGGTCCTTGTTCGT-3') and reverse (5'-TCGACCCGGGAATTCTTAGCCGGGGTAAAGTGGACAATC-3') primers (Oligos Etc., Wilsonville, OR) contained restriction sites (underlined) for *Bam*HI and *Eco*RI, respectively. Recombinant obtustatin molecules contained the additional N-terminal dipeptide (Gly-Ser).

Site-directed mutagenesis was performed by PCR using the pGex-4-T1 vector containing obtustatin as a template and the following primers (Oligos Etc., Wilsonville, OR): mutant (KAS): forward primer 5'-GCTGGCACGACGTGTTGGAAGGCTTCTTACATCC-3' and reverse primer 5'-CTTCCAACACGCGTGCCAGCTGGCTTAAGTTT-3'; mutant (ATS): forward primer 5'-CCAGCTGGCACGACGTGTTGGGCTACATCTTACA-3' and reverse primer 5'-CCAACACGTCGTGCCAGCTGGCTTAAGTTTGCA-3'; mutant (KTA): forward primer 5'-GGCACGACGTGTTGGAAGACAGCTTACATCCCAT-3' and reverse primer 5'-TGCTTCCAACACGTCGTGCCAGCTGGCTTAAG-3'; mutant (AAA): forward primer 5'-CCAGCTGCCACGACGTGTTGGGCTGCTGCTT ACATCCCAT-3' and reverse primer 5'-CCAACA CGTCGTGCCAGCTGGCTTAAGTTTGCA-3'; mutant (KTSR): forward primer 5'-ACGACGTGTTGGAAGACATCTAGAACATCCATTAC-3' and reverse primer 5'-AGATGTCTTCCAACACGTCGTGCCAGCTGGCTT-3'; mutant (KTSA): forward primer 5'-ACGACGTGTTGGAAGACATCTGCTACATCCATTAC-3' and reverse primer 5'-AGATGTCTTCCAACACGTCGTGCCAGCTGGCTT-3'.

The sequences of cDNAs of obtustatin and its mutants were verified at the Kimmel Cancer Center (Thomas Jefferson University, Philadelphia, PA) and used to transform *E. coli* BL21 (DE3) strain. The glutathione S-transferase fusion protein was induced and isolated as described [31]. After digestion with thrombin, recombinant obtustatin and its mutants were purified by reverse-phase HPLC as described [12]. The purity of the recombinant proteins was verified by SDS-PAGE, and Western blot using an anti-eristostatin polyclonal antibody which cross-react with native obtustatin and HRP-based chemiluminescence detection kit (Cell Signaling Inc.).

Cell Adhesion Studies

Cell adhesion studies were performed using an assay developed previously in our laboratory [32]. Briefly, integrin ligands and monoclonal antibody B44 were immobilized on a 96-well plate in PBS (or in 0.02 M acetic acid for collagens I and IV) overnight at 4 °C. Wells were blocked for 1h at room temperature with 1% bovine serum albumin (BSA) in Hanks' balanced salt solution (HBSS) buffer containing 3 mM MgCl₂. Cells were labeled with 12.5 μM of 5-chloromethylfluoresceine diacetate (CMFDA) (Invitrogen, Carlsbad, CA) in HBSS buffer containing 3 mM MgCl₂ for 30 min at 37 °C. Cells were freed from unbound reagent by washing in the same buffer. Labeled cells (1 x 10⁶/ml) suspension were premixed with increasing concentrations of disintegrins, incubated for 15 min at room temperature and added to the wells of the ligand-coated plate. The plate was incubated for 30 min. at 37 °C and unbound cells were removed by washing. Bound cells were lysed by adding 0.5% Triton X-100. In parallel, the

standard curve was prepared in the same plate using known concentrations of labeled cells. Plates were read using an FLx800 (BioTek, Winooski, VT) fluorescence plate reader selecting the bottom reading option, and an excitation wavelength of 485 nm using a 530 nm emission filter.

ELISA

Soluble $\alpha_1\beta_1$ integrin was recombinantly produced in an insect cell expression system and purified as described [33]. Integrin interaction experiments were carried out using an ELISA-type protocol according to [33]. Briefly, the CB3 [IV] collagen fragment was immobilized on a 96-well plate overnight at 4°C in PBS at a concentration of 20 $\mu\text{g/ml}$. The plate was washed three times with TBS, pH 7.5 containing 2 mM MnCl_2 (TBS/Mg) and blocked with 1% BSA in TBS/Mg at room temperature for 1 hour. Then 30 nM of soluble $\alpha_1\beta_1$ integrin, dissolved in the same buffer supplemented with 1 mM MnCl_2 , was mixed with different concentrations of recombinant disintegrins. After incubation for 15 min at room temperature the mixtures were added to the plate and incubated for 2 hours at room temperature. The plate was then washed twice with 50 mM HEPES (pH 7.5) containing 150 mM NaCl , 2 mM MgCl_2 , and 1 mM MnCl_2 , and bound integrin was fixed with 2.5% glutaraldehyde (Sigma Inc.). The $\alpha_1\beta_1$ integrin was detected using a rabbit anti- β_1 antiserum. After washing, goat anti-rabbit IgG conjugated with alkaline phosphatase (AP) was added. 4-Nitrophenyl phosphate disodium salt hexahydrate (Sigma Inc.) was added as a substrate for AP and color was developed at room temperature. The plate was read using ELISA plate reader at 405 nm.

Cell-free disintegrin binding assay for LIBS expression

Disintegrins were labeled with FITC as described [32]. Anti-LIBS monoclonal antibody B44 (0.5 $\mu\text{g/ml}$) or the blocking, conformational insensitive anti- β_1 integrin subunit monoclonal antibody Lia1/2 (0.5 $\mu\text{g/ml}$) were immobilized on 96-well plate. Wells were blocked with 1% BSA as described above (Cell Adhesion Studies). α 1K562 cells were harvested and washed with HBSS containing 3 mM Mg^{2+} . Cell pellet was lysed with 0.5% Triton X-100 in HBSS containing 3 mM Mg^{2+} and protein concentration in the lysate was estimated using the BCA assay kit (Pierce Inc., Rockford, IL). FITC-disintegrin was mixed with cell lysate (2 mg/ml protein) to a total sample volume of 100 μl . Samples were incubated for 30 min at 37 °C and transferred to a 96-well plate with immobilized B44 antibody. To measure unspecific binding of FITC-disintegrin, the same experiment was carried out but using non- α 1-transfected K562 cells. After incubation for 30 min at 37 °C, the plates were washed three times with HBSS containing 3 mM Mg^{2+} and 1 % BSA. Finally, plates were read (bottom reading option) using a fluorescent plate reader FLx800 (BioTek) at an excitation wavelength of 485 nm and a 530 nm emission filter. In parallel, a standard curve of bound disintegrin was prepared on the same plate using known concentrations of FITC-disintegrin.

Molecular modeling

Structure of obtustatin mutants were calculated using NOE information and disulfide bond restraints of the NMR solution structure of obtustatin [1MPZ] and an energy minimization protocol supplied with the program CNS [34]. For the final ensembles, a set of 50 structures was calculated and the converged structures selected corresponded to a plateau in the values of the overall calculated energy. For the analysis of the mutants the lowest energy structure was used as

representative model, and the mutations were introduced using the protocol supplied with the program PyMOL [35] available at <http://www.pymol.org>.

RESULTS

Antagonistic profile of native and recombinant obtustatin

Obtustatin recombinantly produced in *E. coli* exhibited the same chromatographic behavior on reverse phase HPLC as obtustatin purified from viper venom and showed the same inhibitory saturation pattern and IC₅₀ on α 1K562 cell adhesion to immobilized collagen IV as the native (venom-isolated) disintegrin (Fig. 1A, Table 1). The selectivity of recombinant and native obtustatins was also indistinguishable from one another (Fig. 1B). Particularly, neither native nor recombinant obtustatin blocked the adhesive functions of the α ₂ β ₁ integrin that is structurally and functionally highly related to α ₁ β ₁ integrin. The recombinant production of fully active obtustatin allowed us to assess the previously suggested relevance of synthetic KTS-bearing peptides for specific α ₁ β ₁ integrin inhibition [11, 12, 23] employing the site-directed mutated molecules displayed in Fig. 2. Specifically, substitutions within KTS tripeptide motif showed significant impairment of the α ₁ β ₁ integrin inhibitory ability of the recombinant proteins (Fig. 3). Using a cell adhesion assay, the IC₅₀s of the single alanine mutants ²¹ATS²³, KAS, and KTA showed, respectively, 25-fold, 82-fold, and 13-fold decrease inhibiting the α 1K562 cell adhesion to immobilized collagen IV (Fig.3A, Table 1). The triple mutant, ²¹AAA²³, was devoid of inhibitory activity up to a concentration of 10 μ M (Fig.3A, Table 1). Similar features were observed when the single and triple obtustatin mutants were tested for their ability to inhibit the binding of a recombinant soluble form of the α ₁ β ₁ integrin to the CB3 fragment of collagen IV in a cell-free ELISA-type assay (Fig. 3C).

Next, we checked the hypothesis that the residue immediately C-terminal to the KTS motif may be partly responsible for the increased inhibitory potential of viperistatin over obtustatin [12]. To this end, leucine-24 (obtustatin) was replaced for alanine and for arginine (as in viperistatin). The ²¹KTSA²⁴ mutant (Fig.2G) showed only a slight decrease in IC₅₀ in both ELISA-type and cell adhesion assays. On the other hand, the L²⁴/R mutant (Fig.2F) exhibited a 6-fold enhancement in its α ₁ β ₁ inhibitory potential (Table 1) (Fig.3, panels B and C). However, in the adhesion but not in the ELISA-type assay, this latter effect was concentration-dependent since the difference in activity of the KTSR mutant disappeared at disintegrin concentrations higher than 10 nM (compare Figs. 3B and 3C).

KTS-disintegrins induced LIBS epitope upon binding to α 1 β 1 integrin

Ligand engagement to integrins may trigger conformational changes leading to the exposure of cryptic epitopes (LIBS, Ligand-Induced Binding Sites) recognized by monoclonal antibodies [36]. The ability of KTS-disintegrins to induce LIBS was assessed using two different assay systems. Using a solid-phase adhesion assay, we show that both obtustatin and viperistatin significantly induce conformational alterations in α ₁ β ₁ integrin reported by expression of a neoepitope on the β 1 subunit recognized by the B44 monoclonal antibody (Fig. 4A). However, the ability to induce LIBS was significantly lower for viperistatin than for obtustatin. On the other hand, wild-type obtustatin and its KTSR-mutant had similar effects on mAbB44 epitope exposure suggesting that the distinct LIBS-inducing activity of obtustatin and viperistatin may not reside in their integrin-binding loops. On the other hand, using a cell-free binding assay, in

which FITC-labeled disintegrins complexed with $\alpha_1\beta_1$ integrin in the cell lysate were detected following binding to the immobilized B44 antibody, obtustatin, viperistatin and the mutated recombinant KTSR-obtustatin showed similar ability inducing LIBS epitope on $\alpha_1\beta_1$ integrin (Fig. 4B) as in the adhesion assay (Fig. 4A). Binding of FITC-disintegrins to the anti- β_1 blocking antibody Lia1/2, used as a control, was negligible and was subtracted as background from each reading. The outcome of this experimental setup ruled out the possible controversy concerning the possibility that internalization of the ligand/integrin complex influenced the results gathered through the adhesion assay.

DISCUSSION

The $\alpha_1\beta_1$ integrin is widely considered to represent a target for anti-angiogenic, and thus anticancer, therapeutical intervention. Delineating structure-function correlations of specific $\alpha_1\beta_1$ inhibitors is therefore of major pharmaceutical relevance. Our studies using linear synthetic peptides indicated a role for the KTS and RTS tripeptide motifs of obtustatin, viperistatin and jerdostatin in the selective inhibition of integrin $\alpha_1\beta_1$ binding to collagens I and IV *in vitro* [11,12, 26] and angiogenesis *in vivo* [11]. Although not so widely spread among integrin ligands as the RGD tripeptide, the KTS motif is present in human and mouse ADAM-9 disintegrin-like domain at a topologically equivalent position in snake venom disintegrins [37] [UniProtKB/Swiss-Prot entry Q13443]. This motif is also localized in the C-terminal part of VP3, a structural protein of human polyomavirus JC, which after activation induces a multifocal leukoencephalopathy in brain [38]. These findings strongly suggest that the KTS motif may play an important role in certain human pathophysiological conditions. To establish structure-function correlations of KTS-bearing proteins, we have set up a bacterial system for the recombinant expression of fully active obtustatin. A major conclusion from comparison of the $\alpha_1\beta_1$ inhibitory assays using point mutations which gradually converted obtustatin into viperistatin is that substitution of leucine for arginine at position 24, immediately C-terminal to the KTS motif, did not compromise the $\alpha_1\beta_1$ selectivity but accounted for only 40% of the 25-fold enhanced activity of viperistatin over obtustatin. A corollary of this conclusion is that the amino acid adjacent to the KTS motif confers inhibitory potency rather than receptor specificity. Furthermore, the partial enhancement of the inhibitory activity of the KTSR-obtustatin mutant indicated that the other two different residues between viperistatin and obtustatin (L38/V and P40/Q, Fig.2) may contribute to the distinct inhibitory features of KTS-disintegrins.

To provide a structural ground for the functional role of the KTSX motif residues, and to investigate structural determinants of the enhanced inhibitory activity of viperistatin over obtustatin, we generated molecular models of obtustatin and viperistatin (Fig.5). Among the KTS motif residues, mutation of the central threonine-22 for alanine had the major functional impact (Table 1). This effect can be rationalized due to the critical role of this residue to maintain the conformation of the integrin binding loop [23, 28]. A network of interactions between the solvent-shielded $H_{\gamma 2}$ of T22 and residues T25 and S26 explains the restrained mobility of threonine-22 [29]. On the other hand, the 6-fold gain-of-activity conferred by the Leu²⁴/Arg mutation indicates that the positively charged, extended side-chain of arginine is better suited than the solvent-exposed alkyl side-chain of leucine for establishing productive interactions with residues within the ligand-binding site of the $\alpha_1\beta_1$ integrin.

The size and shape of the integrin-binding loop has been proven to be a determinant for conferring integrin specificity to cyclic RGD peptides with a known conformation [39] and to the short-sized RGD-disintegrins echistatin and eristostatin [40]. Thus, the critical importance of T22 may be linked to a structure-stabilizing mechanism of the integrin-binding loop, which supports the correct conformational presentation of the KTS sequence to be recognized by $\alpha_1\beta_1$ integrin, rather than to a direct role in receptor binding.

Though a tripeptide at the tip of a mobile loop represents the primary integrin inhibitory determinant of RGD-disintegrins, both the potency and receptor selectivity of disintegrins appears to be finely tuned by residues flanking the active sequence [16, 40, 41]. Similarly, the presence of arginine at the C-terminal side of the primary KTS integrin-recognition motif of viperistatin enhances its inhibitory activity towards $\alpha_1\beta_1$ integrin by approximately 4-fold in comparison to obtustatin, which contains leucine in this position. However, this non-conservative mutation does not affect the integrin specificity of KTS-disintegrins, whereas structural evidence gathered on synthetic peptides and RGD-disintegrins showed that the amino acid immediately C-terminal to the RGD sequence influence the disintegrin's integrin-recognition selectivity through modulation of the RGD loop conformation [39].

It is also worth noticing that substitution of leucine for arginine at position 24 (sequence F in Fig. 2) was not enough for switching the inhibitory activity of obtustatin to that of viperistatin (Table 1 and Fig. 3B,C). The partial (40%) gain-of-function of recombinant KTSR-obtustatin is in the range of inhibitory activity of lebestatin (IC_{50} , 0.4 nM), another $\alpha_1\beta_1$ -specific KTSR-disintegrin isolated from the venom of *Macrovipera lebetina transmediterranea* [25, 26]. Besides position 24, obtustatin and lebestatin sequences differ only at position 38, which contains Leu and Ser, respectively. In line with structural studies on obtustatin showing that its integrin-binding loop and C-terminal tail displays concerted motions [29] our results suggest that these structural elements act as a secondary determinant of integrin-binding specificity/potency. Relevant to this point, obtustatin and viperistatin have different amino acids at positions 38 and 40, which are L³⁸/V and P⁴⁰/Q, respectively, (Fig. 2). We argue that these two substitutions, along with the active site L²⁴/R mutation, may create a distinct chemical environment responsible for the increased inhibitory activity towards $\alpha_1\beta_1$ integrin of viperistatin over obtustatin. Furthermore, here we show that obtustatin, and to a lower extent viperistatin, elicit the exposure of ligand-induced binding sites (LIBS) in $\alpha_1\beta_1$ recognized by monoclonal antibody B44 (Fig. 4). Our working hypothesis is that proline at position 40 may contribute to the better exposure of conformational changes in the $\alpha_1\beta_1$ -obtustatin complex.

CONCLUDING REMARKS AND SIGNIFICANCE

The $\alpha_1\beta_1$ integrin is an attractive target for the development of novel therapeutical strategies against pathological angiogenesis in cancer and certain inflammatory diseases. The KTSX sequence found in viper venom disintegrins represents a specific motif targeting the $\alpha_1\beta_1$ integrin. The NMR solution structure of the KTS-disintegrin obtustatin along with the structure-function correlations reported here may provide the ground for designing a new generation of synthetic lead compounds with potential application for anti-angiogenic intervention.

A further novel finding of our research is the demonstration that ligand engagement elicits in $\alpha_1\beta_1$ the exposure of cryptic epitopes recognized by monoclonal antibody B44. Ligand-induced binding sites had been reported in β_3 and $\alpha_4\beta_1$ integrins. Our results suggest that

conformational regulation may represent a general feature of integrins for transducing ligand-specific signals. LIBS offer further possibilities for developing immunochemical weapons to fight undesired upregulation of the $\alpha_1\beta_1$ integrin in pathological conditions.

Finally, although our research focused on the structural determinants of snake venom disintegrins for specific inhibition of $\alpha_1\beta_1$ integrin, the occurrence of the KTS tripeptide in certain proteins, such as human ADAM-9 and VP3 capsid protein of the human polyomavirus JC, suggests a hitherto unrecognized role for this motif in physiology and pathophysiology. Functions of ADAM family proteins are not fully characterized. Interactions with collagen receptors may regulate their adhesive and/or enzymatic functions. On the other hand, the presence of KTS sequence on a capsid protein of a virus attacking the human nervous system, suggests that the $\alpha_1\beta_1$ integrin may serve as part of the pathogen's host cell entry strategy. Further investigations on novel KTS-bearing proteins are needed for expanding our understanding of the basic principles underlying its functionality in diverse biological contexts.

ACKNOWLEDGMENTS

This work was supported in part by NIH grant CA100145 (C.M.) and AHA grant 0230163N (C.M.), grant EB177/4-2 from the German Research Council (J.A.E.), and grant BFU2007-61563 from the Ministerio de Ciencia e Innovación, Madrid, Spain (J.J.C.).

REFERENCES

- 1 Calvete, J.J. (1999) Platelet integrin GPIIb/IIIa: structure-function correlations. An update and lessons from other integrins. *Proc. Soc. Exp. Biol. Med.* **222**, 29-38.
- 2 Hynes, R.O. (2002) Integrins: bidirectional, allosteric signaling machines. *Cell* **110**, 673-687.
- 3 Takagi, J. and Springer, T.A. (2002) Integrin activation and structural rearrangement. *Immunol. Rev.* **186**, 141-163.
- 4 Berrier, A.L. and Yamada, K.M. (2007) Cell-matrix adhesion. *J. Cell. Physiol.* **213**, 565-573.
- 5 Luo, B.H., Carman, C.V. and Springer T.A. (2007) Structural basis of integrin regulation and signaling. *Annu. Rev. Immunol.* **25**, 619-647.
- 6 Eble J.A. (2005) Collagen-binding integrins as pharmaceutical targets. *Curr. Pharm. Des.* **11**, 867-880.
- 7 McCall, K.D. and Zutter, M.M. (2008) Collagen receptor integrins: rising to the challenge. *Curr. Drug Targets* **9**, 139-149.
- 8 Hughes, A. L. (2001) Evolution of the integrin α and β families. *J. Mol. Evol.* **52**, 63-72.
- 9 Leitinger, B. and Hogg, N. (1999) Integrin I domains and their function. *Biochem. Soc. Transact.* **27**, 826-832.
- 10 Dickeson, S.K., Mathis, N.L., Rahman, M., Bergelson, J.M. and Santoro, S.A. (1999) Determinants of ligand binding specificity of the $\alpha_1\beta_1$ and $\alpha_2\beta_1$ integrins. *J. Biol. Chem.* **274**, 32182-32191.
- 11 Marcinkiewicz, C., Wainreb, P.H., Calvete, J.J., Kisiel, D.G., Mousa, S.A., Tuszynski, G.P. and Lobb, R.R. (2003) Obtustatin: a potent selective inhibitor of $\alpha_1\beta_1$ integrin in vitro and angiogenesis in vivo. *Cancer Res.* **63**, 2020-2023.
- 12 Kisiel, D.G., Calvete, J.J., Katzhendler, J., Fertala, A., Lazarovici, P., and Marcinkiewicz, C. (2004) Structural determinants of the selectivity of KTS-disintegrins for the $\alpha_1\beta_1$ integrin. *FEBS Lett.* **577**, 478-482.
- 13 Calvete, J.J., Marcinkiewicz, C. and Sanz, L. (2007) KTS and RTS-disintegrins: anti-angiogenic viper venom peptides specifically targeting the $\alpha_1\beta_1$ integrin. *Curr. Pharm. Des.* **13**, 2853-2859.
- 14 Sanz, L., Bazaa, A., Marrakchi, N., Pérez, A., Chenik, M., Bel Lasfer, Z., El Ayeb, M. and Calvete, J.J. (2006) Molecular cloning of disintegrins from *Cerastes vipera* and *Macrovipera lebetina transmediterranea* venom gland cDNA libraries: insight into the evolution of the snake venom integrin-inhibition system. *Biochem. J.* **395**, 385-392.
- 15 Ogawa, T., Chijiwa, T., Oda-Ueda, N. and Ohno, M. (2005) Molecular diversity and accelerated evolution of C-type lectin-like proteins from snake venom. *Toxicon* **45**, 1-14.
- 16 Niewiarowski, S., McLane M.A., Kloczewiak M. and Stewart, G.J. (1994) Disintegrins and other naturally occurring antagonists of platelet fibrinogen receptors. *Semin. Hematol.* **31**, 289-300.
- 17 Marcinkiewicz, C. (2005) Functional characteristic of snake venom disintegrins: potential therapeutic implication. *Curr. Pharm. Des.* **11**, 815-827.
- 18 Calvete, J.J., Marcinkiewicz, C., Monleon, D., Esteve, V., Celda, B., Juarez, P., and Sanz, L. (2005) Snake venom disintegrins: evolution of structure and function. *Toxicon* **45**, 1063-1074.

- 19 Koh, D.C., Armugam, A. and Jeyaseelan, K. (2006) Snake venom components and their applications in biomedicine. *Cell Mol. Life Sci.* **63**, 3030-3041.
- 20 Scarborough, R.M., Rose, J.W., Hsu, M.A., Phillips, D.R., Fried, V.A., Campbell, A.M., Nannizzi, L. and Charo, I.F. (1991) Barbourin. A GPIIb-IIIa-specific integrin antagonist from the venom of *Sistrurus m. barbouri*. *J. Biol. Chem.* **266**, 9359-9362.
- 21 Marcinkiewicz, C., Calvete, J.J., Senadhi, V.K., Marcinkiewicz, M.M., Raida, M., Schick, P., Lobb, R.R. and Niewiarowski, S. (1999) Structural and functional characterization of EMF10, a heterodimeric disintegrin from *Eristocophis macmahoni* venom that selectively inhibits $\alpha_5\beta_1$ integrin. *Biochemistry* **38**, 13302-13309.
- 22 Calvete, J.J., Fox J.W., Agelan, A., Niewiarowski, S. and Marcinkiewicz, C. (2002) The presence of the WGD motif in CC8 heterodimeric disintegrin increases its inhibitory effect on $\alpha_{IIb}\beta_3$, $\alpha_v\beta_3$, and $\alpha_5\beta_1$ integrins. *Biochemistry* **41**, 2014-2021.
- 23 Moreno-Murciano, M.P., Monleón, D.D., Calvete, J.J., Celda, B. and Marcinkiewicz, C. (2003) Amino acid sequence and homology modeling of obtustatin, a novel non-RGD-containing short disintegrin isolated from the venom of *Vipera lebetina obtusa*. *Protein Sci.* **12**, 366-371.
- 24 Brown M.C., Staniszewska I., Del Valle L., Tuszyński G.P. and Marcinkiewicz C. (2008) Angiostatic activity of obtustatin as $\alpha_1\beta_1$ integrin inhibitor in experimental melanoma growth. *Int. J. Cancer* **123**, 2195-2203.
- 25 Bazaa, A., Marrakchi, N., El Ayeb, M., Sanz, L. and Calvete, J.J. (2005) Snake venomics: comparative analysis of the venom proteomes of the Tunisian snakes *Cerastes cerastes*, *Cerastes vipera* and *Macrovipera lebetina*. *Proteomics* **5**, 4223-4235.
- 26 Olfa, K.Z., José, L., Salma, D., Amine, B., Najet, S.A., Nicolas, A., Maxime, L., Raoudha, Z., Kamel, M., Jacques, M., et al. (2005) Lebestatin, a disintegrin from *Macrovipera* venom, inhibits integrin-mediated cell adhesion, migration and angiogenesis. *Lab Invest.* **85**, 1507-1516.
- 27 Sanz, L., Chen, R.Q. Perez, A., Hilario, R., Juarez, P., Marcinkiewicz, C., Monleon, D., Celda, B., Xiong, Y.L., Pérez-Payá, E. and Calvete, J.J. (2005) cDNA cloning and functional expression of jerdostatin, a novel RTS-disintegrin from *Trimeresurus jerdonii* and a specific antagonist of the $\alpha_1\beta_1$ integrin. *J. Biol. Chem.* **280**, 40714-40722.
- 28 Moreno-Murciano, M.P., Monleón, D. Marcinkiewicz, C., Calvete, J.J. and Celda, B. (2003) NMR solution structure of the non-RGD disintegrin obtustatin. *J. Mol. Biol.* **329**, 135-145.
- 29 Monleón, D., Moreno-Murciano, M.P., Kovacs, H., Marcinkiewicz, C., Calvete, J.J. and Celda, B. (2003) Concerted motions of the integrin-binding loop and the C-terminal tail of the non-RGD disintegrin obtustatin. *J. Biol. Chem.* **278**, 45570-45576.
- 30 Bazan-Socha, S., Kisiel, D.G., Young, B., R. Theakston, R.D.G., Calvete, J.J., Sheppard, D. and Marcinkiewicz, C. (2004) Structural requirements of MLD-containing disintegrins for functional interaction with $\alpha_4\beta_1$ and $\alpha_9\beta_1$ integrins. *Biochemistry* **43**, 1639-1647.
- 31 Smith, D.B. and Johnson, K.S. (1988) Single-step purification of polypeptides expressed in *Escherichia coli* as fusions with glutathione S-transferase. *Gene* **67**, 31-40.
- 32 Marcinkiewicz, C., Vijay-Kumar, S., McLane, M. A. and Niewiarowski, S. (1997) Significance of RGD loop and C-terminal domain of echistatin for recognition of $\alpha_{IIb}\beta_3$ and $\alpha_v\beta_3$ integrins and expression of ligand-induced binding site. *Blood* **90**, 1565-1575.

- 33 Eble, J. A., Kassner, A., Niland, S., Morgelin, M., Grifka, J. and Grassel, S. (2006) Collagen XVI harbors an integrin $\alpha_1\beta_1$ recognition site in its C-terminal domains. *J. Biol. Chem.* **281**, 25745-25756.
- 34 Brunger, A.T., Adams, P.D., Clore, G.M., DeLano, W.L., Gros, P., Grosse-Kunstleve, R.W., Jiang, J.S., Kuszewski, J., Nilges, M., Pannu, N.S., Read, R.J., Rice, L.M., Simonson, T. and Warren, G.L. (1998) Crystallography & NMR system: A new software suite for macromolecular structure determination. *Acta Crystallogr. D Biol. Crystallogr.* **54**, 905-921.
- 35 DeLano, W.L. (2002) The PyMOL Molecular Graphics System, DeLano Scientific, Palo Alto, CA, USA.
- 36 Humphries, M.J. (2004) Monoclonal antibodies as probes of integrin priming and activation. *Biochem. Soc. Trans.* **32**, 407-411
- 37 Weskamp, G., Krätzschmar, J., Reid, M.S. and Blobel, C.P. (1996) MDC9, a widely expressed cellular disintegrin containing cytoplasmic SH3 ligand domains. *J. Cell Biol.* **132**, 717-726.
- 38 Trowbridge, P.W. and Frisque, R.J. (1995) Identification of three new JC virus proteins generated by alternative splicing of the early viral mRNA. *J. Neurovirol.* **1**, 195-206.
- 39 Pfaff, M., Tangemann, K., Müller, B., Gurrath, M., Müller, G., Kessler, H., Timpl, R. and Engel, J. (1994) Selective recognition of cyclic RGD peptides of NMR defined conformation by $\alpha_{IIb}\beta_3$, $\alpha_v\beta_3$ and $\alpha_5\beta_1$ integrins. *J. Biol. Chem.* **269**, 20233-20238.
- 40 McLane, M.A., Vijay-Kumar, S., Marcinkiewicz, C., Calvete, J.J. and Niewiarowski, S. (1996) Importance of the structure of the RGD-containing loop in the disintegrins echistatin and eristostatin for recognition of $\alpha_{IIb}\beta_3$ and $\alpha_v\beta_3$ integrins. *FEBS Lett.* **391**, 139-143.
- 41 Lu, X., Rahman, S., Kakkar, V.V. and Authi, K.S. (1996) Substitutions of proline 42 to alanine and methionine 46 to asparagine around the RGD domain of the neurotoxin dendroaspin alter its preferential antagonism to that resembling the disintegrin elegantin. *J. Biol. Chem.* **271**, 289-294.

LEGENDS TO FIGURES

Figure 1. Comparison of the effect of recombinant and native obtustatin on integrin-mediated cell adhesion to different ECM proteins.

ECM proteins (2 $\mu\text{g/ml}$) were immobilized overnight at 4°C on a 96-well plate in 0.02 M acetic acids for collagen and in PBS for VCAM-1 and fibronectin. After blocking the plate with BSA, CMFDA-labeled cells preincubated in the presence or absence of snake venom proteins were added to the wells, and incubated for 30 min at 37°C. Non-binding cells were washed out, adhered cells were lysed, and the plate was read using a fluorescence plate reader. (Panel A) Effect of different concentrations of recombinant and native obtustatin on inhibition of adhesion of $\alpha 1\text{K562}$ cells to collagen IV. (Panel B) Effect of recombinant (a) and native (b) obtustatin, VP12 (c), VLO5 (d) and VLO4 (e) on adhesion of the indicated cell lines to their respective immobilized ligands. Venom proteins were applied at a concentration of 20 $\mu\text{g/ml}$. VP12 belongs to subgroup of snake venom C-type lectin-like proteins that specifically target the $\alpha_2\beta_1$ integrin [50]. VLO5 and VLO4 are dimeric disintegrins from *V.l. obtusa* which antagonize the function of integrins $\alpha_4\beta_1$ and $\alpha_4\beta_1$, respectively [30, 51]. The observed small inhibition activity of native obtustatin on $\alpha_4\beta_1$ integrin binding to VCAM-1 was due to a slightly contamination with VLO5 which has almost identical reverse-phase retention time as obtustatin. Error bars represent S.D. from three independent experiments.

Figure 2. Amino acids sequences of obtustatin and its mutants recombinantly expressed in *E. coli*.

Mutated residues are in boldface. A, wild-type obtustatin; sequences B – E, mutants affecting the KTS motif; sequences F – H, mutations for converting obtustatin into viperistatin.

Figure 3. Effect of recombinant obtustatin and its mutants on the interaction of $\alpha 1\beta 1$ integrin with collagen IV.

(Panel A) Effect of wild-type obtustatin and its KTS motif mutants on the adhesion of $\alpha 1\text{K562}$ cells to immobilized collagen IV. (Panel B) Effect of wild-type viperistatin and obtustatin and the KTSA and KTSR mutants on the adhesion of $\alpha 1\text{K562}$ cells to immobilized collagen IV. (Panel C) Effect of wild-type obtustatin and its mutants on the binding of soluble $\alpha_1\beta_1$ integrin to immobilized CB3 fragment of collagen IV using the ELISA-type assay described in the Experimental Procedures section. Error bars represent S.D. from three experiments.

Figure 4. Effect of wild-type viperistatin and obtustatin and the KTSR-obtustatin mutant on LIBS expression.

In panel A, experiments were performed using cell adhesion assays. To this end, monoclonal antibody B44 recognizing a LIBS epitope on the $\beta 1$ subunit was immobilized on a 96-well plate (0.5 $\mu\text{g/ml}$) by overnight incubation at 4 °C in PBS. After blocking the plate with BSA, CMFDA-labeled $\alpha 1\text{K562}$ cells preincubated in the presence (1 mM in HBSS containing 3 mM Mg^{2+}) or absence of disintegrins were added and incubated at 37°C for 30 min. Unbound cells were removed by washing, adhered cells were lysed with 0.5% Triton X-100, and fluorescence was read using a fluorescence plate reader. The error bars represent S.D. from three experiments.

(*) Represents statistical difference between control and samples incubated with disintegrins, as determined by unpaired T-test ($p < 0.05$). (**), Statistical difference between samples incubated

with wild-type or mutated obtustatin molecules and with viperistatin ($p < 0.05$). In panel **B**, experiments were performed using a cell-free binding assay. α 1K562 cells were lysed with HBSS containing 3 mM Mg^{2+} and 0.5% Triton X-100. FITC-disintegrins were mixed with 100 μ l of cell lysate (2mg/ml) for 30 min at 37 °C followed by incubation for another 30 min at 37 °C with monoclonal antibody B44 immobilized on the wells of a 96-well plate. The same experiment was carried out using the lysate of non-transfected K562 cells as a control of the specific binding of the FITC-disintegrin to integrin $\alpha_1\beta_1$ (\blacklozenge). After washing with HBSS containing 3 mM Mg^{2+} fluorescence was read using a fluorescence plate reader. Error bars represent S.D. from three independent experiments.

Figure 5. Molecular models of obtustatin and viperistatin.

(Panel **A**) NMR solution structure of obtustatin (1MPZ) showing the locations of residues (rendered in stick representation) which were sequentially mutated in the different recombinant proteins shown in Fig. 2 to convert recombinant obtustatin into viperistatin. (Panel **B**) Computer modelling of the transformation of obtustatin into viperistatin. Figures were rendered using PyMol.

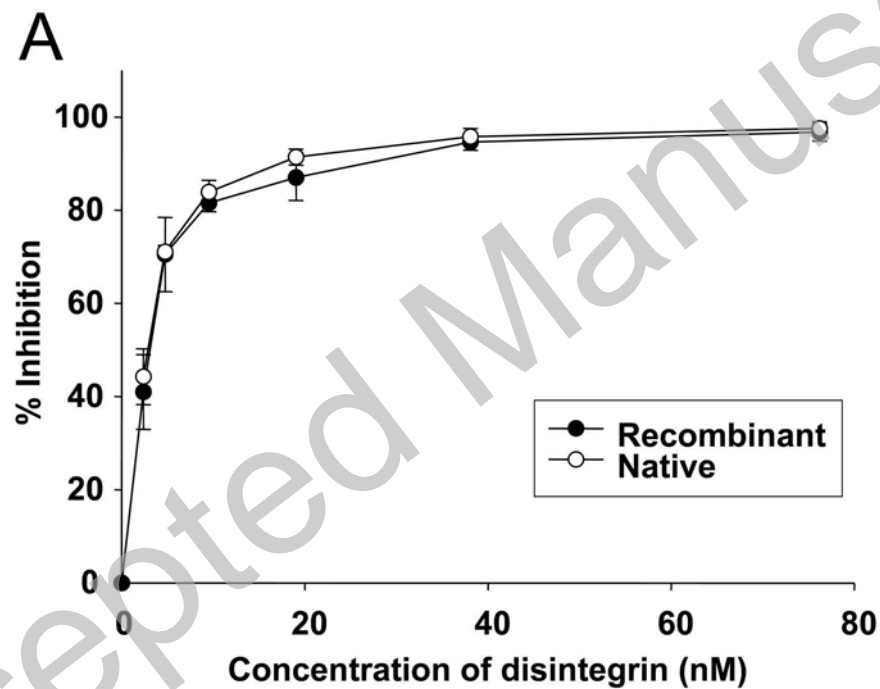
TABLE 1

Inhibition of α 1K562 cell adhesion to immobilized collagen IV by wild-type obtustatin and viperistatin and the different obtustatin mutants.

Type of mutation	IC ₅₀ (nM) [†]
Wild-type recombinant/native obtustatin	2.00
Wild-type native viperistatin	0.08
ATS-obtustatin	51.30
KAS-obtustatin	164.18
KTA-obtustatin	26.08
AAA-obtustatin	>10,000
KTSR-obtustatin	0.33
KTSA-obtustatin	2.56

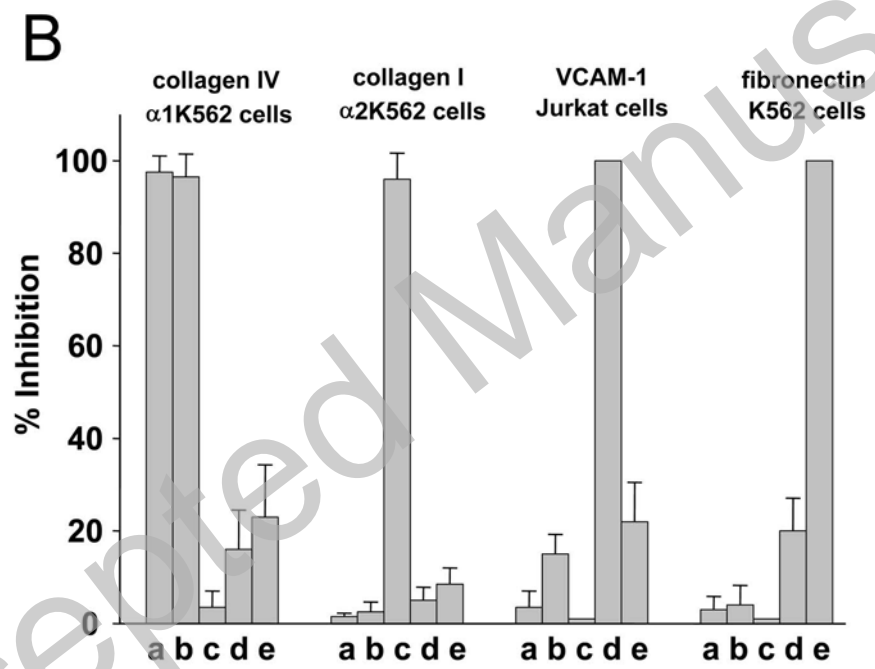
[†] Data represent mean from three independent experiments

Figure 1



THIS IS NOT THE VERSION OF RECORD - see doi:10.1042/BJ20081403

Figure 1



THIS IS NOT THE VERSION OF RECORD - see doi:10.1042/BJ20081403

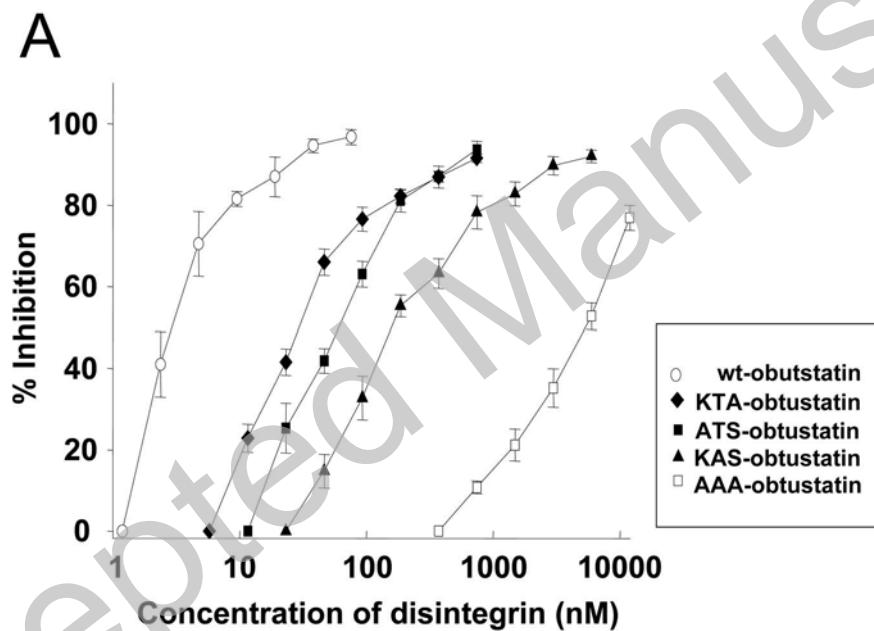
Figure 2

Active site


A	<u>C</u> <u>T</u> <u>T</u> <u>G</u> <u>P</u> <u>C</u> <u>C</u> <u>R</u> <u>Q</u> <u>C</u> <u>K</u> <u>L</u> <u>K</u> <u>P</u> <u>A</u> <u>G</u> <u>T</u> <u>T</u> <u>C</u> <u>W</u>	K T S	<u>L</u> <u>T</u> <u>S</u> <u>H</u> <u>Y</u> <u>C</u> <u>T</u> <u>G</u> <u>K</u> <u>S</u> <u>C</u> <u>D</u> <u>C</u>	<u>P</u> <u>L</u> <u>Y</u> <u>P</u>	G
B	<u>C</u> <u>T</u> <u>T</u> <u>G</u> <u>P</u> <u>C</u> <u>C</u> <u>R</u> <u>Q</u> <u>C</u> <u>K</u> <u>L</u> <u>K</u> <u>P</u> <u>A</u> <u>G</u> <u>T</u> <u>T</u> <u>C</u> <u>W</u>	A T S	<u>L</u> <u>T</u> <u>S</u> <u>H</u> <u>Y</u> <u>C</u> <u>T</u> <u>G</u> <u>K</u> <u>S</u> <u>C</u> <u>D</u> <u>C</u>	<u>P</u> <u>L</u> <u>Y</u> <u>P</u>	G
C	<u>C</u> <u>T</u> <u>T</u> <u>G</u> <u>P</u> <u>C</u> <u>C</u> <u>R</u> <u>Q</u> <u>C</u> <u>K</u> <u>L</u> <u>K</u> <u>P</u> <u>A</u> <u>G</u> <u>T</u> <u>T</u> <u>C</u> <u>W</u>	K A S	<u>L</u> <u>T</u> <u>S</u> <u>H</u> <u>Y</u> <u>C</u> <u>T</u> <u>G</u> <u>K</u> <u>S</u> <u>C</u> <u>D</u> <u>C</u>	<u>P</u> <u>L</u> <u>Y</u> <u>P</u>	G
D	<u>C</u> <u>T</u> <u>T</u> <u>G</u> <u>P</u> <u>C</u> <u>C</u> <u>R</u> <u>Q</u> <u>C</u> <u>K</u> <u>L</u> <u>K</u> <u>P</u> <u>A</u> <u>G</u> <u>T</u> <u>T</u> <u>C</u> <u>W</u>	K T A	<u>L</u> <u>T</u> <u>S</u> <u>H</u> <u>Y</u> <u>C</u> <u>T</u> <u>G</u> <u>K</u> <u>S</u> <u>C</u> <u>D</u> <u>C</u>	<u>P</u> <u>L</u> <u>Y</u> <u>P</u>	G
E	<u>C</u> <u>T</u> <u>T</u> <u>G</u> <u>P</u> <u>C</u> <u>C</u> <u>R</u> <u>Q</u> <u>C</u> <u>K</u> <u>L</u> <u>K</u> <u>P</u> <u>A</u> <u>G</u> <u>T</u> <u>T</u> <u>C</u> <u>W</u>	A A A	<u>L</u> <u>T</u> <u>S</u> <u>H</u> <u>Y</u> <u>C</u> <u>T</u> <u>G</u> <u>K</u> <u>S</u> <u>C</u> <u>D</u> <u>C</u>	<u>P</u> <u>L</u> <u>Y</u> <u>P</u>	G
F	<u>C</u> <u>T</u> <u>T</u> <u>G</u> <u>P</u> <u>C</u> <u>C</u> <u>R</u> <u>Q</u> <u>C</u> <u>K</u> <u>L</u> <u>K</u> <u>P</u> <u>A</u> <u>G</u> <u>T</u> <u>T</u> <u>C</u> <u>W</u>	K T S	R <u>T</u> <u>S</u> <u>H</u> <u>Y</u> <u>C</u> <u>T</u> <u>G</u> <u>K</u> <u>S</u> <u>C</u> <u>D</u> <u>C</u>	<u>P</u> <u>L</u> <u>Y</u> <u>P</u>	G
G	<u>C</u> <u>T</u> <u>T</u> <u>G</u> <u>P</u> <u>C</u> <u>C</u> <u>R</u> <u>Q</u> <u>C</u> <u>K</u> <u>L</u> <u>K</u> <u>P</u> <u>A</u> <u>G</u> <u>T</u> <u>T</u> <u>C</u> <u>W</u>	K T S	A <u>T</u> <u>S</u> <u>H</u> <u>Y</u> <u>C</u> <u>T</u> <u>G</u> <u>K</u> <u>S</u> <u>C</u> <u>D</u> <u>C</u>	<u>P</u> <u>L</u> <u>Y</u> <u>P</u>	G
H	<u>C</u> <u>T</u> <u>T</u> <u>G</u> <u>P</u> <u>C</u> <u>C</u> <u>R</u> <u>Q</u> <u>C</u> <u>K</u> <u>L</u> <u>K</u> <u>P</u> <u>A</u> <u>G</u> <u>T</u> <u>T</u> <u>C</u> <u>W</u>	K T S	R <u>T</u> <u>S</u> <u>H</u> <u>Y</u> <u>C</u> <u>T</u> <u>G</u> <u>K</u> <u>S</u> <u>C</u> <u>D</u> <u>C</u>	P V Y Q	G

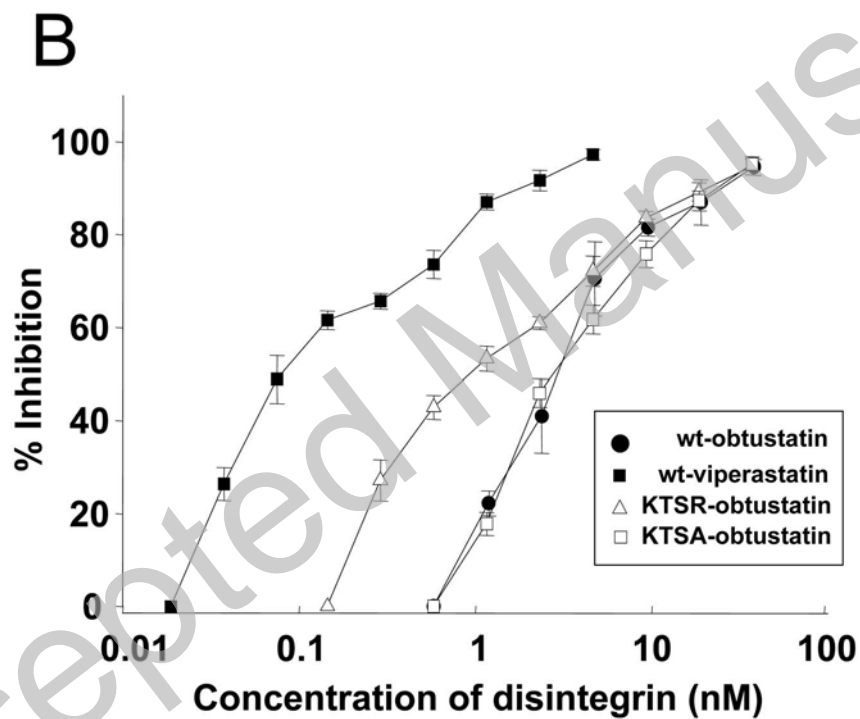
THIS IS NOT THE VERSION OF RECORD - see doi:10.1042/BJ20081403

Figure 3



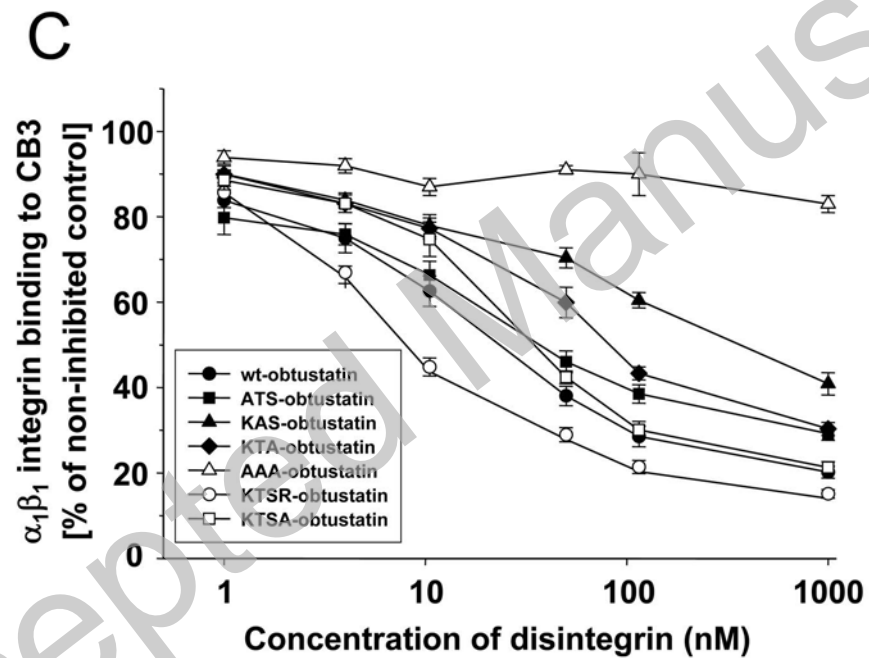
THIS IS NOT THE VERSION OF RECORD - see doi:10.1042/BJ20081403

Figure 3



THIS IS NOT THE VERSION OF RECORD - see doi:10.1042/BJ20081403

Figure 3



THIS IS NOT THE VERSION OF RECORD - see doi:10.1042/BJ20081403

Figure 4

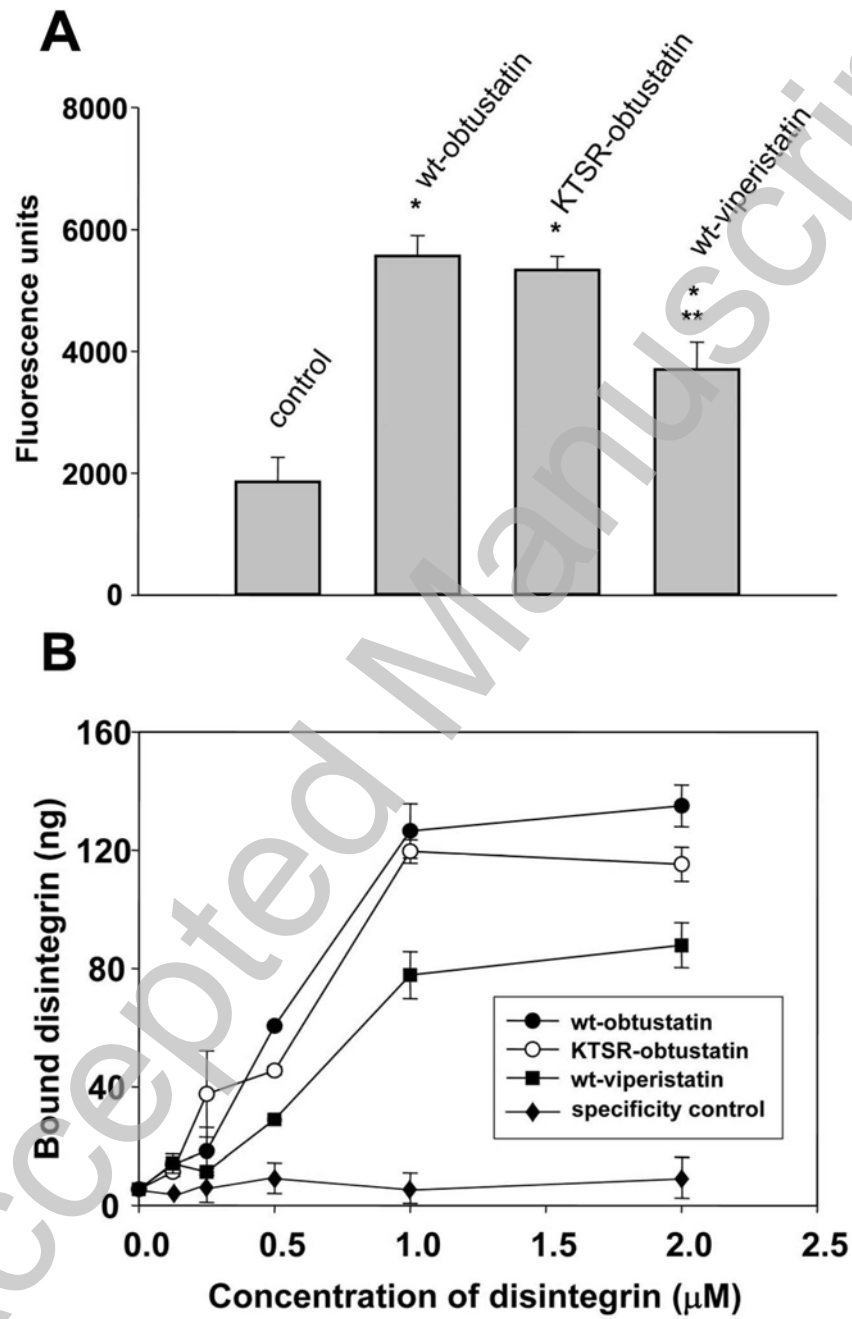
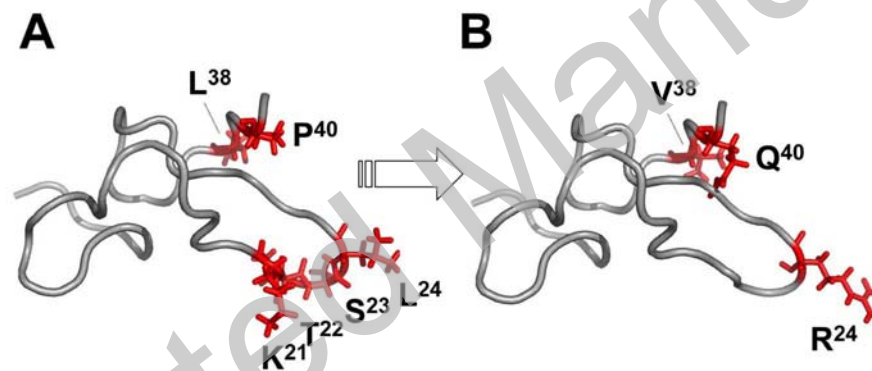


Figure 5



THIS IS NOT THE VERSION OF RECORD - see doi:10.1042/BJ20081403